

Towards a Soft Exosuit for Hypogravity Adaptation: Design and Control of Lightweight Bubble Artificial Muscles

Emanuele Pulvirenti^{1,2}, Richard S. Diteesawat^{1,3}, Helmut Hauser^{1,3}, Jonathan Rossiter^{1,3}

Abstract—Lower body soft exosuits have been shown to improve the capabilities of humans in a wide range of applications, from rehabilitation to worker enhancement. Their light weight and ability to be easily sewn into fabrics make them attractive for both terrestrial and space exploration applications. One unaddressed challenge in space exploration is the prevalence of low (hypo) gravity conditions, which can have a serious deleterious effect on the human body. To address this challenge we propose the hypogravity exosuit (or HEXsuit), which can help maintain the physical fitness and health of inter-planetary travellers. A core component of the HEXsuit is compliant, comfortable and efficient soft robotic artificial muscles. A recently proposed pneumatic actuator, the Bubble Artificial Muscle (BAM), is particularly suited for integration into hypogravity exosuits. In this work we explore the design and control of lightweight BAM actuators. Characterisation results show that a thin actuator is capable of high contraction, while a thicker actuator can be used for high load applications. Two control modes were implemented: displacement control and force control. Both controllers achieve low steady state error and show high accuracy. The displacement controller is also shown to be capable of maintaining the required displacement while actively changing external loads, a typical use case within the proposed hypogravity HEXsuit.

Soft Robotics, Bubble Artificial Muscles, pneumatic, artificial muscle, exoskeleton, exosuit, space exploration

I. INTRODUCTION

Lower body assistive devices have been shown to improve the capabilities of humans in a wide range of applications, from rehabilitation after injury or stroke to performance augmentation in factories and for soldiers [2]. Most lower body assistive devices available on the market are rigid [3] and can provide high torques. These devices therefore require high level of control for safety issues [4], and this increases complexity and reduces the speed of operation. Recent advances in soft robotics have made soft lower body exosuits a valid alternative to rigid ones. Soft robotic elements, such as artificial muscles, soft pumps and soft sensors, represent a viable alternative to conventional rigid components such as motors, gears and solenoids. Their potential integration

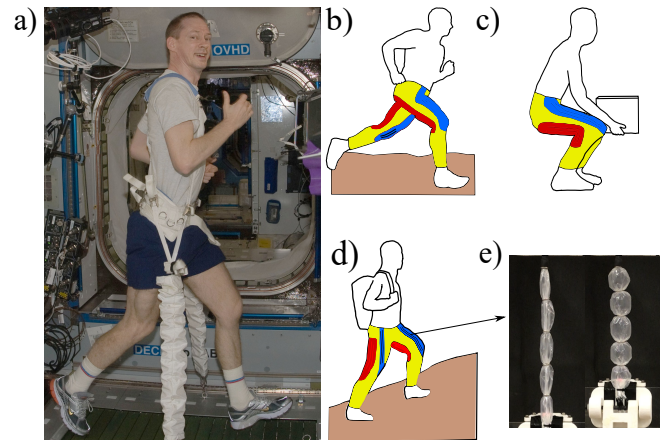


Fig. 1: a) Current countermeasures to hypogravity effects include a strict two-hour daily exercise routine. (Reproduced from [1]). b-d) Conceptual design of the HEXsuit and typical uses on Mars. Blue and red areas illustrate antagonist pairs of actuators placed at the hamstrings and quadriceps muscles. Inset photo e) shows the actuation of the Bubble Artificial Muscle as a core actuator in the HEXsuit in relaxed (left) and contracted (right) states.

into soft exosuits enables the design of a new generation of devices which resemble clothes that the user can wear comfortably [5]. In addition to the significant need for assistive mobility devices for healthcare, applications off-planet also require the development of new devices and tools. These include planned manned missions to planets and moons within the solar system. A round-trip to Mars, with time to undertake experiments, may take between 18 months and two years. These hypogravity conditions (very low in transit, and approximately 1/3 Earth's gravity when on Mars) are expected to have significant negative effects on the bodies of astronauts. Effects include loss of muscle mass, osteoporosis and arrhythmogenesis [6].

Lower body assistive devices have been designed for space applications to counteract the detrimental effects of microgravity on astronauts' health [7]–[9], along with a daily exercise routine (see Fig.1a). Rigid exoskeletons, for example the X1 [10], were explored to enhance the exercise routine of International Space Station (ISS) crewmembers, but could not be used during Extra Vehicular Activities (EVAs). Additionally, rigid exoskeletons require precise control of the robotic joints to allow smooth interaction with the user and might prove to be difficult to operate in a constrained space

¹Bristol Robotics Laboratory, UK.

²EPSRC Centre for Doctoral Training in Robotics and Autonomous Systems (FARSCOPE), University of Bristol and University of the West of England, UK.

³Department of Engineering Mathematics, University of Bristol, UK.

EP and HH were funded by the Engineering and Physical Sciences Research Council (EPSRC) grant EP/S021795/1. RSD was supported by EPSRC grant EP/S026096/1. JR was supported by EPSRC grants EP/L015293/1, EP/R02961X/1, EP/V026518/1, and EP/T020792/1, and the Royal Academy of Engineering through the Chair in Emerging Technologies scheme.

such as the ISS.

Soft exosuits represent an attractive solution to the challenges posed by space applications, thanks to their low weight, cost and power requirements. Soft exosuits, like the Skinsuit [11] that provides passive axial loading to simulate Earth's gravitational pull, were developed to address muscle deterioration. However, the comfort and full performance of the Skinsuit are still to be tested. The predominant common feature of these uses is a low, or hypo, gravity. As such, a new type of soft exosuit, tailored to low gravity is required. We term such a device a hypogravity exosuit, or HEXsuit.

To enable the application of soft exosuits in extraterrestrial hypogravity, one can first look at Earth. Several designs exist and are usually cable or pneumatically driven devices [12]–[16]. While cable-driven devices present the most constrained behaviour of the two and can be made compliant through complex control strategies, pneumatic actuators present high strength-to-weight ratio and are inherently compliant [17]. A recently proposed pneumatic actuator called the Bubble Artificial Muscle (BAM) [18] has particularly high potential for use in such suits. It produces higher relative contractions than traditional McKibben actuators and operates at a lower pressure than other existing soft actuators such as the cylindrical soft actuators (CSAs) presented in [19] and extensor bending pneumatic artificial muscles (EBPAMs) [20]. This increases safety and range of applications. Additionally, BAM actuators present higher force-to-weight ratio ($\approx 321\text{N/g}$ vs. 211.5N/g of CSAs, for example) when compared to other pneumatic artificial muscles.

The work presented in this paper focuses on the characterisation and control of two designs of BAMs for HEXsuit applications: one for high tensile strength and one for high contraction. The aim is to develop two control modes that allow for: (i) displacement control, i.e. controlling how the muscle contracts, and (ii) force control, i.e. controlling how much force the muscle should produce, both of which, for this type of actuator, have previously been unaddressed. The paper is organised as follows. In Section II, the actuator characterisation is presented. A series of isotonic tests were performed to assess the contraction range of thick and thin BAM actuators under different loading conditions. The control strategy design and the results showing the performance of each controller are presented in Section III and IV. Finally, conclusions and future work are discussed in Section V.

II. ACTUATORS CHARACTERISATION

A. Design and Fabrication

Bubble Artificial Muscles (BAMs) are fabricated by inserting thin plastic tubing through regularly-spaced narrow metal retaining rings [18]. The tubing is flexible but inextensible. The rings act to constrain the actuator shape, creating folds of tubing membrane around the rings. When inflated, the membrane unfolds causing simultaneous radial expansion and coupled actuator contraction (inset in Fig. 1).

In this work, two different types of BAM were designed by using different material thicknesses; actuators made of thin and thick membranes to deliver high contraction or high

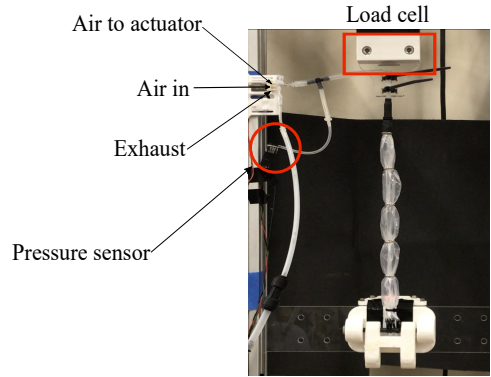


Fig. 2: Experimental rig physical setup

tensile strength, respectively. The prototypes were fabricated following the directions and principles introduced in [18]. These two actuator designs operate near the centre of the BAM performance landscape; the performance of BAMs is dependant on contractile unit length l (defined as the region between two metal rings), ring radius r , and material thickness t . Table I presents the characteristics of the thin and thick BAM actuators. The material used to fabricate the actuators was low-density polyethylene (Young's Modulus $E = 0.3$ GPa). In the present study, these parameters were selected to fit the chosen application. When walking in hypogravity ($0.31g$ the peak moment at the knee to be expected is within the range of $18.74\text{ Nm} - 26.25\text{ Nm}$ (for a 75 kg subject) [22]. From previous applications of the BAMs [21] we know that actuators with similar parameters are capable of delivering 2.73 Nm of assistive moment at the knee. A single BAM could hence provide between $14.5\% - 10.4\%$ of the total moment required.

TABLE I: Characteristics of the two BAM actuators

	$t(\text{mm})$	$l(\text{mm})$	$r(\text{mm})$
Thin BAM actuator	0.030	48.0	2.9
Thick BAM actuator	0.125	48.0	4.5

B. Experimental Setup

Both types of actuators consisted of five contractile units in series, as shown in Fig. 2. A series of isotonic experiments was performed to determine the maximum contraction achievable, while the pressure and the load applied were held constant. Each actuator was placed vertically in a testing rig (Fig. 2) with the inlet end attached to an acrylic mount linked to a 1 kN load cell (700 Series S Beam Load Cell, Load Cell Shop, UK). The other end of the actuator was attached to a slider of mass 0.328 Kg , which was used as a displacement reference to measure the actuator stroke by means of a laser displacement sensor (LK-G507, Keyence). Both actuators were tested under a range of constant pressures and loads presented in Table II. Compressed air was supplied to the actuator through a three-head electric air compressor. A manual

TABLE II: Range of test conditions for isotonic tests

	Pressures (kPa)	Loads (N)
Thin BAM	10, 15, 20	3.23, 4.20, 6.17, 7.15, 8.13
Thick BAM	20, 30, 40, 50	3.23, 8.13, 13.04, 15.00, 16.96

regulator attached to the rig was used to regulate the pressure delivered to the actuator. A three-way solenoid valve (S070C-SBG-32; Best Pneumatic Systems) was used to control the air flow to the actuator, controlled by a relay module (4 Channel 5V 10A Relay Module; Elegoo) that was commanded by a NI Data Acquisition device (USB-6211; National Instruments). Pressure was measured using a differential pressure sensor (SSCDRRV015PDAA5; Honeywell).

C. Experimental procedure

Both actuators were tested five times for each pressure and loading setting in isotonic experiments. Each test was 18 seconds long; the valve was opened for 9 seconds to allow full expansion of the actuator membrane and the pressure to converge to a constant value, and then the exhaust was open for 9 seconds, allowing the actuator to relax completely and return to its original shape before performing the next test. Pressure and displacement data were collected throughout the duration of each test. The contraction c of the actuator was calculated as follows:

$$c = \frac{\bar{d} - \bar{m}_{in}}{L}, \quad (1)$$

where \bar{d} is the mean value of maximum measured displacement, calculated over the 5 trials of each test condition. \bar{m}_{in} is the mean starting position, and L is the total length of the actuator ($L = l \times 5 \text{ units} = 240 \text{ mm}$).

D. Characterisation results

The isotonic results of both BAM types are presented in Fig. 3. It was found that the thin actuator was able to operate at pressure up to 20 kPa, showing a maximum contraction of 26% (62.4 mm) when no weight was attached to the slider (the load is only from the 0.3 kg slider). In contrast, the thick actuator was able to operate up to 50 kPa, delivering a maximum contraction of 22.5% (54.0 mm) under the same loading condition. Additionally, the thin actuator was able to withstand a maximum testing load of 8.1 N, whereas the thick actuator was able to sustain a heavier testing load of up to 17 N. These limits are defined as the maximum load at which no further contraction was detected.

The tests showed a standard deviation from the mean between $\pm 0.3\%$ and $\pm 1\%$ with the exception of the tests performed for the thin actuator at 20 kPa when supporting a 6.2N tensile load. The trials in this experiment showed a $\pm 1.3\%$ standard deviation from the mean. This might be due to non-uniform unfolding of the folded membrane, thus influencing the performance of the actuator. The next section describes the two control modes designed for these actuators, assessing the performance of each controller.

III. CONTROL STRATEGY

A. Control hardware

An Arduino Uno microcontroller was used to control the airflow in and out the BAMs by means of two solenoid valves (VDW250-5G-2-01F-Q, SMC). One valve was used to inflate the actuator, whereas the other exhausted air from the actuator. The displacement and pressure were measured using the same sensors as described above. All signals from the load cell (1022M-5M-F-106, Tedea-Huntleigh), laser displacement sensor, pressure sensor and valves were recorded using the data acquisition device at a sampling frequency of 1 kHz. The control loop on the Arduino board ran every 5 ms. Both the displacement and force controllers were implemented as an Arduino IDE script, written in C, and a PID control strategy was designed for both.

B. Displacement control loop design

The desired set point $r(t)$ (demand) for the displacement controller was set by the user (from 5 to 60 mm for the thin actuator and 5 to 30 mm for the thick actuator). The process variable $y(t)$ was the measured contraction of the actuator, and the control output $u(t)$ was the duty cycle of the inlet and exhaust valves. This was controlled using the *analogWrite* function of the Arduino microcontroller, which maps the 0-100% duty cycle range to a 0-255 range. For this reason, the output of the PID was scaled accordingly to fit this range of values. The control loop was designed as follows:

- The demand $r(t)$ (in mm) was pre-set according to the experimental protocol;
- The PID control loop ran every 5 ms, calculating the error $e(t) = r(t) - y(t)$ between the demand and the output of the displacement sensor $y(t)$;
- The scaled PID output $u(t)$ was sent to the relays that controlled the valves. A signal with duty cycle proportional to the PID output was sent to the relays

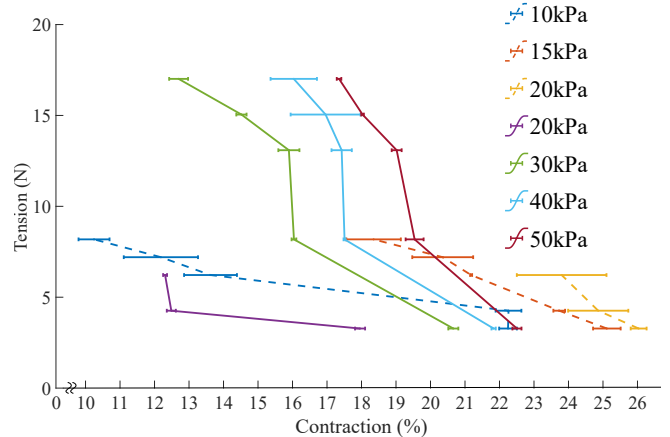


Fig. 3: Results of isotonic tests; dashed lines represent results for the thin actuator ($t = 0.030 \text{ mm}$), and solid lines represent results for the thick actuator ($t = 0.125 \text{ mm}$)

through the *analogWrite* function, effectively controlling the opening rate of the valves.

- An allowable error threshold was empirically found, different for each actuator (± 1 mm and ± 0.8 mm for thin and thick actuators, respectively). This was set to avoid oscillation around the set point, given the binary nature of the output signal (valve open/closed). In the simplest controller embodiment, the inlet valve opened while the measured displacement $y(t)$ was below the lower threshold limit, and the exhaust valve was opened when $y(t)$ exceeded the upper limit; if $y(t)$ was within the threshold, both valves were closed.

The controller was tuned following the Ziegler–Nichols (ZN) method presented in [23], aiming at minimising the overshoot of the system. Equation 2 presents the tuning rules using this method. K_u and T_u are defined as a critical gain and a critical period, respectively. K_u was found to be the minimum proportional gain that caused steady and consistent oscillations in the system, while T_u is the critical period of the oscillation produced. The gains obtained were used as a starting point and then manually tuned. Table IV presents the gains obtained using the ZN method.

$$\begin{aligned} K_P &= 0.2K_u \\ K_D &= 0.066(K_u T_u) \\ K_I &= 0.4 \left(\frac{K_u}{T_u} \right) \end{aligned} \quad (2)$$

TABLE III: PID gains (K_P, K_D, K_I) for displacement controller

	ZN gains	Manually tuned gains
Thin BAM actuator	0.400, 0.148, 0.722	0.1, 0.5, 0.3
Thick BAM actuator	0.8, 0.227, 1.877	2, 5, 0.5

C. Weight disturbance experiment

To demonstrate that the controller allows for precise displacement control even under changing load conditions, a weight disturbance experiment was performed on both actuators. A demand was set at 15 mm, and progressively heavier weights were manually attached to the slider at regular intervals (≈ 5 s). The range of weights used for the thin actuator were 0.1, 0.2, 0.3 and 0.4 kg, while a set of 0.5, 0.6, 0.7, 0.8 kg were used for the thick actuator.

D. Force control loop design

The force controller was designed following the same framework outlined for the displacement controller, with the exception that the user-set demand (from 3 to 15 N for the thin actuator and from 5 to 25 N for the thick actuator) was now compared to the data acquired from the load cell. To test the force controller, the displacement of the BAM actuator was adjusted by attaching it to a linear displacement actuator.

TABLE IV: PID gains (K_P, K_D, K_I) for force controller

	ZN gains	Manually tuned gains
Thin BAM actuator	0.4, 0.148, 0.722	10, 0, 0.001
Thick BAM actuator	0.8, 0.227, 1.877	7, 0, 0.001

IV. RESULTS AND DISCUSSION

A. Controller performance

The performances of both controllers were evaluated according to their time response characteristics. Fig. 4a and 4b present the results for a range of demands for displacement and force respectively. The rise time of both actuators under both controlling conditions was satisfactory for HEXsuit applications, with the force controller maintaining a rise time of less than 1s (Fig. 4b, left). The rise time for the displacement controller of the thick actuator was consistently smaller than 1s, whereas that of the thin actuator was up to 2.45s (Fig. 4a, left). This could be because when higher demands were approached (i.e. 40, 45, 50 and 60 mm), the thin actuator approached the maximum operating pressure (20 kPa) and allowable contraction, meaning that the final steps needed to achieve the required demand were taken at a slower rate.

One of the objectives of controller tuning was to minimise the overshoot. The overshoot of the displacement controller for the thick actuator show a decreasing trend as the demand increases, reducing from 60.9% at 5-mm demand to 3.7% at 30-mm demand (Fig. 4a, middle). The thin actuator, in general, showed smaller values of overshoot with a maximum of 21%. In contrast, the force controller performed better in terms of overshoot, with values for the thick actuator below 11%, while the thin actuator showed a maximum overshoot of 21% (Fig. 4b, middle). The oscillations found in the overshoot values of the thin actuator highlight one limitation of the controller implementation so far considered; the performance of the controller was hampered by the dynamics dependant on the physical design of the actuator.

As previously stated, the non-uniform shapes of the folded and inflated membrane may be introducing undesired non-zero inputs that modify the effect of the controller on the actuator. This means that every time the test rig and the actuator were reset to repeat a test for a different demand, the initial conditions of the membrane changed, thus affecting the repeatability of the actuator response. However, when used within the HEXsuit, the actuators can be used in an antagonistic configuration, with one actuator assisting knee flexion and one driving knee extension. This configuration would allow the actuator to stretch completely after every actuation cycle and go back to a more repeatable initial condition, thus providing a more reliable and consistent response to the control input. This will be investigated in the future.

In terms of steady-state error, both controllers performed well with errors contained within ± 0.8 mm and ± 0.8 N (within user-set thresholds), showing high accuracy. The steady-state error of the thick actuator for a force demand of

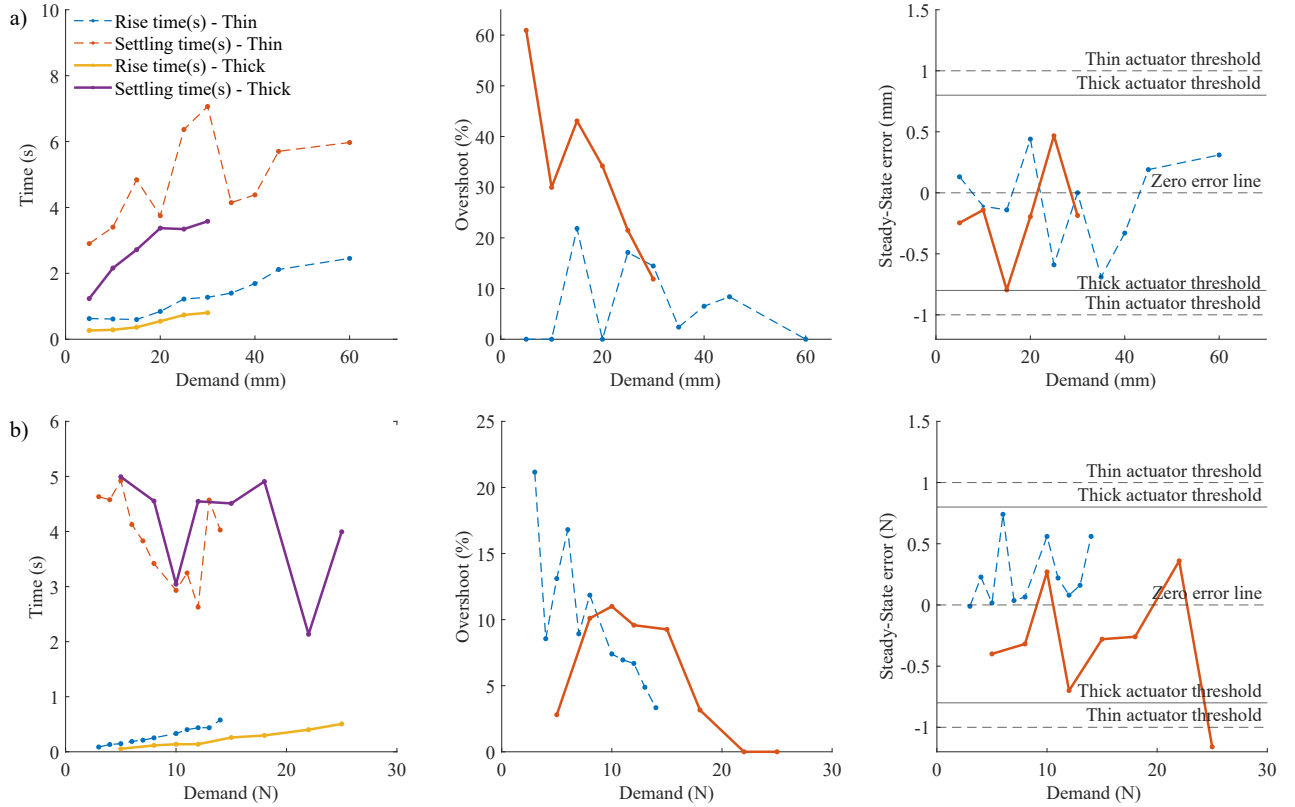


Fig. 4: Time response characteristics for both control modes; *dashed* lines represent results for the thin actuator and *solid* lines represent results for the thick actuator. a) Performance of the displacement controller. b) Performance of the force controller (demands refer to force developed by the actuator). Figures a) and b) share the same legend.

25 N exceeded the threshold boundaries (Fig. 4b, right); this is due to the fact that at this stage the actuator had reached its maximum pressure at 50 kPa before achieving the demand requested.

B. Pressure supply effect

Another factor that might influence the actuator response is the level of pressure that is supplied to the system. The results shown in Fig. 5 suggest that the supply pressure influences the overshoot induced. This data suggests that if overshoot effects are to be minimised, the system should run at low supply pressures (20-30 kPa in this case). This range of pressures is suited to actuation of the thin actuator, but it will reduce the maximum available contraction of the thick actuator by about 4%. For space applications in hypogravity (such as Mars' gravity, which is equal to 38% of Earth's gravity) this is acceptable, as lower rates of muscle contraction and less abrupt gait transitions are to be expected [24].

C. Weight disturbance experiment results

The results for this experiment are presented in Fig. 6 as time-domain plots of key input, output and control values. Here, the behaviour of the thin actuator under changing load conditions shows that the controller was able to adjust for the weights and maintain the required displacement. When the

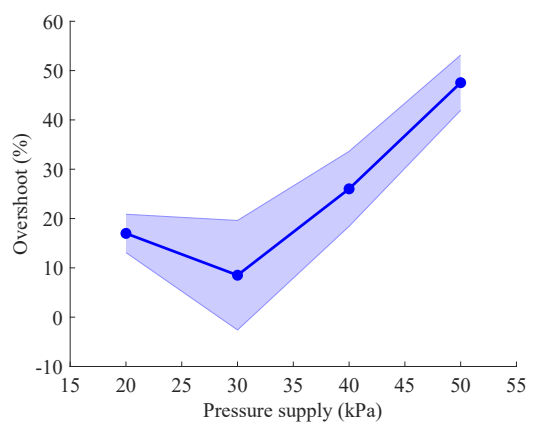


Fig. 5: Effect of pressure supply level on the overshoot response of the system (demand = 15 mm, thick actuator). The data was obtained for 5 trials at each pressure.

weight was taken off, the actuator resettled to its original position. This provides scope for the proposed HEXsuit application where the assistance required by the user is constantly changing, requiring the actuator to be adaptable to a variety of demands.

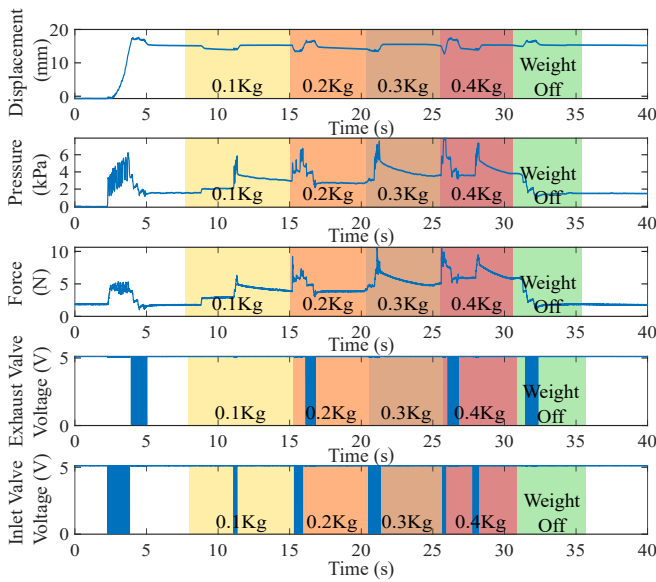


Fig. 6: Results of the weight disturbance experiment
(Demand = 15mm, Thin actuator).

V. CONCLUSION

This paper introduced a first control strategy to be implemented for Bubble Artificial Muscles with the aim of integrating them within the proposed HEXsuit. Two actuators made of different membrane thickness were designed and characterised, each exhibiting different qualities in terms of operating pressure, contraction and generated force. Two control modes – displacement and force control – were presented to provide multiple options of controlling the assistance delivered by the HEXsuit. It was found that with the present design, the actuators are strain and history dependant; however, they present qualities that make them attractive for space applications. They are lightweight and can be easily integrated in the fabric of a soft exosuit without impairing the astronaut's movement. They can also provide assistance at low pressures, which translates to low power requirements.

This work provides a preliminary understanding of how the BAM actuators interact with a controller and their current limitations. In future, to avoid folding issues, the actuators could be fabricated with pre-folded material to allow control over the shape of the actuator at all stages of actuation and increased repeatability. Moreover, a configuration where multiple actuators are placed in parallel could produce more predictable behaviour by compensating for variations in the response of each actuator. This configuration will be the object of future investigations.

The next stage of this study will focus on the application of more advanced control techniques. Since the performance of the actuator depends on the shape of the membrane and supply pressure, an adaptive controller could yield more fitting time response characteristics. Additionally, a more accurate assessment of the dynamic characteristics of the actuator will be performed, to produce an accurate description of the

model plant.

REFERENCES

- [1] Wikipedia contributors. "Effect of spaceflight on the human body." Wikipedia, The Free Encyclopedia. Wikipedia, The Free Encyclopedia, 9 Oct. 2021. Web. 29 Oct. 2021.
- [2] Yan, Tingfang, et al. "Review of assistive strategies in powered lower-limb orthoses and exoskeletons." *Robotics and Autonomous Systems* 64 (2015): 120-136.
- [3] Guizzo, Erico, and Harry Goldstein. "The rise of the body bots [robotic exoskeletons]." *IEEE Spectrum* 42.10 (2005): 50-56.
- [4] Schiele, André, and Frans CT Van der Helm. "Influence of attachment pressure and kinematic configuration on pHRI with wearable robots." *Applied Bionics and Biomechanics* 6.2 (2009): 157-173.
- [5] Asbeck, Alan T., et al. "Stronger, smarter, softer: next-generation wearable robots." *IEEE Robotics & Automation Magazine* 21.4 (2014): 22-33.
- [6] Fong, Kevin. "The next small step." *BMJ* 329.7480 (2004): 1441-1444.
- [7] Bloomberg, Jacob J., et al. "Risk of impaired control of spacecraft/associated systems and decreased mobility due to vestibular/sensorimotor alterations associated with space flight." No. JSC-CN-34446. 2015. (2015)
- [8] DiZio, Paul, and James R. Lackner. "Motion sickness susceptibility in parabolic flight and velocity storage activity." *Aviation, space, and environmental medicine* 62.4 (1991): 300-307.
- [9] Lacquaniti, Francesco, et al. "Human locomotion in hypogravity: from basic research to clinical applications." *Frontiers in physiology* 8 (2017): 893.
- [10] Rea, Rochelle, et al. "X1: A robotic exoskeleton for in-space countermeasures and dynamometry." *AIAA Space 2013 Conference and Exposition*. 2013.
- [11] Carvil, Philip A., et al. "The effect of the gravity loading countermeasure skinsuit upon movement and strength." *The Journal of Strength & Conditioning Research* 31.1 (2017): 154-161.
- [12] Panizzolo, Fausto A., et al. "A biologically-inspired multi-joint soft exosuit that can reduce the energy cost of loaded walking." *Journal of Neuroengineering and Rehabilitation* 13.1 (2016): 1-14.
- [13] Kim, Jinsoo, et al. "Reducing the metabolic rate of walking and running with a versatile, portable exosuit." *Science* 365.6454 (2019): 668-672.
- [14] Wehner, Michael, et al. "A lightweight soft exosuit for gait assistance." *2013 IEEE international Conference on Robotics and Automation*. IEEE, (2013).
- [15] Lotti, Nicola, et al. "Adaptive model-based myoelectric control for a soft wearable arm exosuit: A new generation of wearable robot control." *IEEE Robotics & Automation Magazine* 27.1 (2020): 43-53.
- [16] Sridar, Saivimal, et al. "A soft-inflatable exosuit for knee rehabilitation: Assisting swing phase during walking." *Frontiers in Robotics and AI* 5 (2018): 44.
- [17] Daerden, Frank, and Dirk Lefever. "Pneumatic artificial muscles: actuators for robotics and automation." *European Journal of Mechanical and Environmental Engineering* 47.1 (2002): 11-21.
- [18] Ditesawat, Richard Suphapol, et al. "Characteristic analysis and design optimization of bubble artificial muscles." *Soft Robotics* 8.2 (2021): 186-199.
- [19] Thalman, Carly M., et al. "A novel soft elbow exosuit to supplement bicep lifting capacity." *2018 IEEE/RSJ International Conference on Intelligent Robots and Systems (IROS)*. IEEE, 2018.
- [20] Al-Fahaam, Hassanin, Steve Davis, and Samia Nefti-Meziani. "The design and mathematical modelling of novel extensor bending pneumatic artificial muscles (EBPAMs) for soft exoskeletons." *Robotics and Autonomous Systems* 99 (2018): 63-74.
- [21] Ditesawat, Richard Suphapol, et al. "High strength bubble artificial muscles for walking assistance." *2018 IEEE International Conference on Soft Robotics (RoboSoft)*. IEEE, 2018.
- [22] MacLean, Mhairi K., and Daniel P. Ferris. "Human muscle activity and lower limb biomechanics of overground walking at varying levels of simulated reduced gravity and gait speeds." *PloS one* 16.7 (2021): e0253467.
- [23] McCormack, Anthony S., and Keith R. Godfrey. "Rule-based autotuning based on frequency domain identification." *IEEE Transactions on Control Systems Technology* 6.1 (1998): 43-61.
- [24] Labini, Francesca Sylos, et al. "Smooth changes in the EMG patterns during gait transitions under body weight unloading." *Journal of Neurophysiology* 106.3 (2011): 1525-1536.